Growth, Structure, Spectral Characterization, Fluorescence and Thermal Studies on Phenyltrimethylammonium Trichloro Cadmiate (II) Crystals

V. Mohanraj[1*], M. Thenmozhi[3], R. Pavithra[2], Jaslin J. Christopher[1], A. S. Jebamalar[4], R. Umarani[2]

[1]Department of Chemistry, Manonmaniam Sundaranar, University Constituents College, Kanniyakumari, TN, India
[2]Department of Chemistry, Government Arts College (Autonomous), Coimbatore, TN, India
[3]Department of Physics, Bangalore City College, Bangalore, KA, India
[4]Department of Physics, Nesamony Memorial Christian College, Marthandam, TN, India

ABSTRACT

Crystallography is a fascinating division of the entire study of the optical technology. The single crystal of Phenyl trimethyl ammonium trichloro cadmiate (II) crystals [PTMAC (II)] was grown by slow evaporation technique at room temperature. The grown crystals were characterized using CHN analysis, FT-IR, ^{1}H NMR spectra to confirm with functional groups and structures in spectroscopy methods. TG/TDA analysis were used to find out the thermal stability of grown crystals and fluorescence studies were also carried out, followed by single crystal X-ray diffraction studies by using SHELXL and refined by full matric latest square methods. The molecule belongs to monoclinic crystal system with C_2i/n space group. Focus has been laid on the phase transition of crystals which makes the study interesting; moreover, inorganic crystals are being used for many applications in the field of computer technology.

Keywords: FT-IR; ^{1}H NMR; Single crystal X-ray diffraction; TG/DTA.

1. INTRODUCTION

Crystal growth is an inter-disciplinary field covering Physics, Chemistry, Material Science, Chemical Engineering, Metallurgy, Geology, Crystallography, Mineralogy and Molecular Biology. Crystals are known to man from the earlier period. Many forms of solid matter are crystalline in nature. Orderly arranged atoms, ions or molecules in crystalline solids provide shining appearance and coloured crystals which are still more attractive. The art of growing crystals has always been fascinating and challenging. Modern technology requires semiconductors, magnetic garnets, solid state lasers, and ultraviolet and infrared which in turn requires nano-level materials in good crystalline form (Gesi, 1986). Crystals of good quality in suitable size and perfection are required in technologically important fields like electronic industries, computer technologies, fibre optic communications and ferroelectric materials (Fousek, 1991; Ishibashi *et al.* 1986).

Rapid advances in microelectronics, communication technologies, medical instrumentations and energy and space technologies are possible simply because of

remarkable progress in the fabrication of large and rather perfect crystals (Strukov, 1989; Shimomura *et al.* 1995; Asahi and Hasebe, 1994; Hasebe *et al.* 1994; Heine and Mc Connel, 1984). Crystals are pillars of modern technology. If not for the crystals, there would be no electronic industry, photonic industry and fibre optic communications (Kasano *et al.* 1992; Dvorak and Kind, 1981; Kahirizi and Steinitz, 1989). Crystals have an important role in the production of highly effective light emitting diodes. Energy saving illumination and photovoltaic devices for transforming solar and other radiation into electric power with high yield depend on significant advances in crystal growth (Sato *et al.* 1986; Kapustianik *et al.* 1995; Sawada *et al.* 1978; Mashiyama *et al.* 1980). The significance of the crystals for a technological society and the development of scientific knowledge has been realized. The inorganic and organic crystals are differing in fundamental way from gases, liquids and solids. The grown crystals with more components have an important role in several industrial and optical applications (Mohanraj *et al.* 2019). Fluorescence compounds are widely useful in chemico-physico sensors and fluorescent labeling. Phenyl groups are excellent chromospheres and their metal complexes

show strong light-emitting properties and fluorescence with long durability (Subashini and Arjun, 2018; Peer Mohamed *et al.* 2019).

2. EXPERIMENTAL PROCEDURES

Single crystals of Phenyl trimethyl ammonium trichloro cadmiate (II) [PTMATCl-Cd (II)] crystals were grown by slow evaporation method at room temperature. The compound was prepared by mixing phenyl trimethyl ammonium chloride and cadmium chloride in 1:1 molar ratio using triply distilled water as the solvent. The two solutions were mixed thoroughly. In order to maintain acidic medium and to avoid hydrolysis, 1 ml of HCl is added. The resulting solution was filtered using the Whatmann paper 42. The filtrate collected in a beaker was covered by a filter paper with minute pores and kept at room temperature for the preparation of crystal by slow evaporation. The crystals thus obtained were colourless and transparent.

The compound was obtained according to the following chemical equation:

$$[C_6H_5(CH_3)_3N]Cl + CdCl_2 \xrightarrow{H_2O/ HCl} [C_6H_5(CH_3)_3N]CdCl_3$$
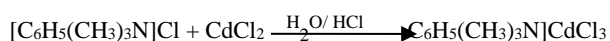
(Phenyl trimethylammonium trichloro cadmiate (II) crystal)

3. RESULTS AND DISCUSSION

3.1 Elemental Analysis

The result of elemental analysis (C, H and N) of crystals and the comparison of theoretical values and experimental values are given in the Table 1. The experimental values of Carbon, Hydrogen and Nitrogen were very close to the theoretical values based on ABX_3 formula. The elemental analysis thus confirmed the stoichiometry of the PTMATCl-Cd (II) compound. This technique was used to find out Carbon, Hydrogen and Nitrogen elements' percentages and other elements were calculated.

Table 1. CHN Analysis of PTMATCl – Cd (II) crystals

Sample	Carbon %		Hydrogen %		Nitrogen %	
PTMACL -Cd[II]	Exp.	Theo.	Exp.	Theo.	Exp.	Theo.
	30.40	30.42	4.19	3.94	3.94	3.94

3.2 FT-IR Spectrum

The FTIR spectra of PTMATCl-Cd (II) is shown in the Fig. 1. The various absorption frequencies

and their assignments are presented in the Table 2. The peak at 3044.32 cm^{-1} was due to Ar-H stretching vibrations of phenyl group. The peak at 1594.91 cm^{-1} was due to C-N bending mode. The peak at 1490.57 cm^{-1} was due to C-H in-plane asymmetric bending due to methyl group. The peak at 1460.70 cm^{-1} was due to C-H bending deformation mode of methyl group. The peak at 949.61cm^{-1} was due to C-H out of plane bending vibration. The peak at 843.61 cm^{-1} was due to C-H deformation out of plane vibration. The peak at 757.44 cm^{-1} was due to aromatic in-plane bending vibration and meta di-substituted aromatic ring stretching. This region was helpful in identifying the type of substitution on aromatic ring. C-N-C and C-C-N deformation modes and di-substituted meta-C-H deformation were seen at 685.50 cm^{-1}.
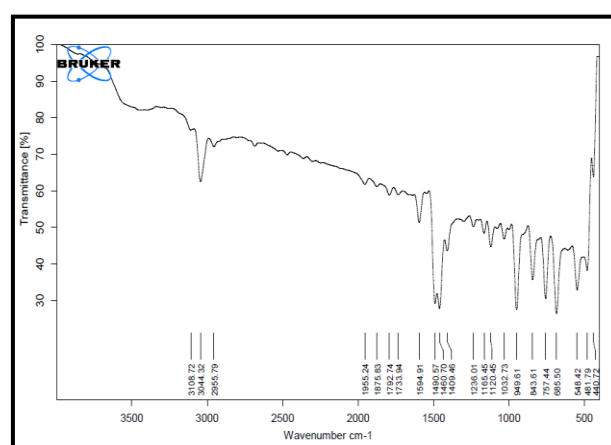
Fig. 1: FTIR Spectrum of PTMATCl-Cd (II) crystals

Table 2. FTIR spectral data for PTMATCl-Cd (II) crystals

S. No.	Frequency (cm^{-1})	Assignment
1.	3044.32	Ar-H stretching vibrations of phenyl group
2.	1594.91	C-N bending mode
3.	1490.57	C-H in-plane asymmetric bending due to methyl group
4.	1460.70	C-H bending deformation mode of methyl group
5.	949.61	C-H out of plane bending vibration
6.	843.61	C-H deformation out of plane vibration
7.	757.44	Aromatic in-plane bending vibration, meta di-substituted aromatic ring stretching
8.	685.50	C-N-C and C-C-N deformation modes.

3.3 ^{1}H NMR Spectroscopy

The normal ^{1}H NMR spectrum of PTMATCl-Cd (II) crystals is shown in Fig. 2. The structure of PTMATCl-Cd [II] compound is $C_6H_5(CH_3)_3NCdCl_3$. In this spectrum, four signals were observed at different δ values for the methyl and Ar-H groups were present in the compound. All the methyl and Ar-H groups were in the same environment. The expected δ values for methyl and aromatic protons are 1.2 to 1.4 ppm and 7.5 to 7.8 ppm. In this spectrum, higher δ value was obtained. This was due to the de-shielding effect which confirms the presence of positive charge on the nitrogen containing three methyl groups and Ar-H groups. The signal at 3.6 δ was due to the presence of methyl group protons. The intensity of the peak was higher due to methyl proton. The peak at 7.9 δ was due to Ar-H protons and it splits into a triplet. The peak at 7.9 δ splits into a triplet due to an aromatic proton. The peak at 7.6 δ splits into a triplet due to an aromatic proton.

Therefore, IR spectral analysis of PTMATPCl-Cd (II) has confirmed the presence of fundamental groups of various bonding vibration of the compound. The Cd-Cl bond was a weak bond vibration and hence these frequencies occured in the Far IR region.

Fig. 2 ^{1}HNMR Spectrum of PTMATCl-Cd (II) crystals

3.4 Thermogravimetry - Differential Thermal Analysis (TG-DTA)

The TG-DTA thermogram of the compound phenyl trimethylammonium trichloro cadmiate (II) crystals is shown in Fig. 3. The compound was subjected to uniform heating of 20 ℃ / minute in a nitrogen atmosphere. The TG-DTA curve showed a two-stage weight loss when heated between the room temperature and 800 ℃. The first stage decomposition started at 180 ℃ and ended at 536 ℃. There was a weight loss of 49.63% which can be accomplished by formulating the

following decomposition reaction of the compound. When the compound undergoes decomposition as above, one mole of the compound decomposes into one mole of phenyl trimethylammonium chloride and one mole of cadmium chloride. Since $[C_6H_5(CH_3)_3N]CdCl_3$ was stable at these temperatures, it does not vaporize at these temperatures. The theoretical loss of 49.63% is observed whereas the experimental loss observed was 48.36%. The difference is 1.29% which indicated that the experimental and theoretical values are close to each other and the result was within the experimental error.

$$[C_6H_5(CH_3)_3N]CdCl_3 \xrightarrow{49.65\%} [C_6H_5(CH_3)_3N]Cl + CdCl_2 \uparrow$$

$$354.97 \qquad\qquad 171.67 \quad 183.3$$

In the second stage, there was only one mole of cadmium chloride that decomposes at 524 ℃. When the temperature increased, there was decomposition of $CdCl_2$ from 524 ℃ to 699 ℃ with a weight loss of 50.47%. This weight loss can be accounted for by formulating the following reaction:

$$CdCl_2 \xrightarrow{50.47\%} CdCl_2 \uparrow$$

$$183.3 \qquad\qquad 183.3$$

The experimental weight loss was 50.47%, whereas the theoretical weight loss was 51.6%. The difference (1.13%) indicated that the experimental and theoretical values were close to each other and the result was within the experimental error. The theoretical residual mass was 0.1%. Experimentally, there is no residue. Thus the compound decomposes in two stages. The decomposition starts at 180 ℃ and gets completed at 700 ℃. Thus, the thermogram has confirmed the stoichiometry of the compound which was evident from the decomposition patterns.

Fig. 3: TG-DTA spectrum of PTMATCl-Cd (II) crystals

3.5 Fluorescence studies

The emission of the light which dwindles due to the excitation in cut-off is due to fluorescence. Fluorescence is a physico-chemical property which occurs in molecules that are aromatic compounds and contains multiple conjugated double bonds with a high degree of resonance stability. The Fluorescence spectrum of PTMATCl-Cd (II) crystal was measured to confirm the emission spectrum concerned with that particular excited state of the system. The Fluorescence emission spectrum of PTMATCl-Cd (II) crystal is shown in Fig. 4. The observed emission peak with maximum intensity at 534 nm has shown that the crystal exhibited green colour fluorescence emission; the existence of only one sharp peak has indicated good crystalline perfection.
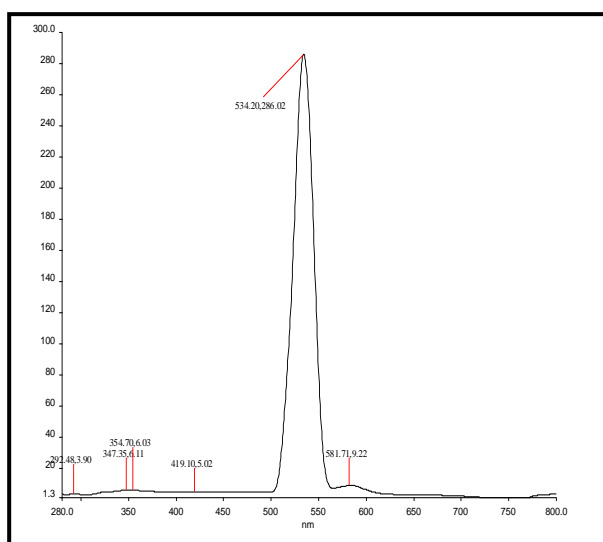
Fig. 4: Fluorescence spectrum of PTMATCl-Cd (II) crystals

3.6 Single crystal X-ray Structural analysis of PTMATCl-Cd (II) Crystals

The structure of the compound was determined by single crystal X-ray diffraction technique. The X-ray data for the compound were collected at 293 K using the M_oK_α radiation ($\lambda = 0.71073A^o$). The unit cell parameters of the crystal were determined by least square using several reflections. The structure was solved by using SHELXL and refined by full matrix least square method. The intensity data were collected for h = -16 to 17, k = -14 to 19, l = -9 to 9. The crystal structure data for the grown crystal is presented in Table 3.

The C-N-C bond angles are given in Table 3. There was no greater deviation when the bond angles were around the normal tetrahedral angle of 109.5°. In some cases observed from the Tables 2-11, the bond angles were lesser than the normal tetrahedral angle, while in some other cases the bond angles were greater than the normal tetrahedral angle, indicating a steric and electronic strain around these groups.

Table 3. Crystal structure data of PTMATCl – Cd (II) crystals

|	
Empirical formula	$C_9 H_{14} Cd Cl_3 N$
Formula weight	354.96
Temperature	293(2) K
Wavelength	0.71073 A
Unit cell dimensions	a = 12.7634(3) A alpha = 90 deg. b = 14.4964(5) A beta = 96.375(5) deg. c = 7.1365(7) A gamma = 90 deg. $\alpha=\gamma=90^o$, $\beta\neq90^o$
Space group crystal system	P21/n Monoclinic
Volume	1312.25(14) A^{o3}
Z, Calculated density	4, 1.797 Mg/m^3
Absorption coefficient	2.239 mm^{-1}
F(000)	696
Theta range	2.13 to 28.49 deg.
Limiting indices	$-16\leq h \leq17$ $-14\leq k\leq19$ $-9\leq l \leq 9$
Reflections collected / unique	6080 / 2733 [R(int) = 0.0328]
Completeness to theta = 25.00	99.90%
Refinement method	Full-matrix least-squares on F^2
Data / restraints / parameters	2733 / 2 / 130
Goodness-of-fit on F^2	1.06
Final R indices [I>2sigma(I)]	R1 = 0.0697, wR2 = 0.2041
R indices (all data)	R1 = 0.0706, wR2 = 0.2057
Absolute structure parameter	0.09 (9)
Largest diff. peak and hole	5.987 and -1.600 eA^{-3}

Table 4. Bond angles for C-N-C

Group	Bond angle (°)
C(9)-N(1)-C(6)	110.9(10)
C(9)-N(1)-C(7)	111.0(11)
C(6)-N(1)-C(7)	109.3(10)
C(9)-N(1)-C(8)	107.2(13)
C(6)-N(1)-C(8)	111.7(11)
C(7)-N(1)-C(8)	106.8(13)

Table 5. Bond angles for H-C-H

Group	Bond angle (°)
H(7A)-C(7)-H(7B)	109.5
H(7A)-C(7)-H(7C)	109.5
H(7B)-C(7)-H(7C)	109.5
H(8A)-C(8)-H(8B)	109.5
H(8A)-C(8)-H(8C)	109.5
H(8B)-C(8)-H(8C)	109.5
H(9A)-C(9)-H(9B)	109.5
H(9A)-C(9)-H(9C)	109.5
H(9B)-C(9)-H(9C)	109.5

In majority of the H-C-H groups, the tetrahedral angle observed was exactly 109.5° which indicates the ideal tetrahedral nature of the bonds in all these groups. These groups were not at all affected by any strain present in the compound. In the case of some other H-C-H groups, the deviation was very minimum showing again the tetrahedral nature of the groups. The bond angles have suggested that all the bond angles were nearly tetrahedral. The C-C-N bond angles are given in Table 6. The variation in the bond angles were due to varying degrees of steric and electronic repulsions around the phenyl group in the positive ion; also, the nitrogen was positively charged and the N-C bond was not completely covalent in nature. From Table **7,** it has been very clear that the C-C-C bond angles were nearly tetrahedral in many of the C-C-C groups. In certain cases, there was an increase in the bond angle. For C(4)-C(3)-C(2), the bond angle was 121°. This increase from the normal tetrahedral angle was attributed to steric and electronic repulsion around these groups from the bond angles shown in Table 8. It is very clear that all the bond angles were nearer to the normal tetrahedral angle of 109.5°. Hence it was obvious that there is no distortion in the tetrahedral symmetry of the C-C-H groups. In the CdCl$_3$ tetrahedral group, a bond length of 2.429A° to 2.847A° was observed for all the Cd-Cl bonds. The Cd-Cl bond length was greater than C-H, C-N and C-C bond lengths. The hydrogen bonds present between the hydrogen of the methyl group and chlorine of the CdCl$_3$ group led to a stronger interaction between the Ar-N and CdCl$_3$. The structure of cobalt compound is [C$_6$H$_5$(CH$_3$)$_3$N]CdCl$_3$. From Table 8, it was very clear

that all the C-C bonds have more or less the ideal bond length. The very small differences may be due to the strain in their environment.
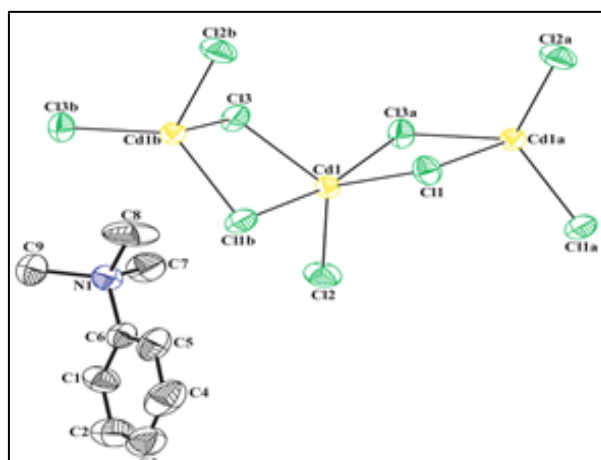
Fig. 5: ORTEP plot of PTMATCl – Cd (II) crystals

The C-H bond length in phenyl groups were 0.93 while it was 0.96 for all the methyl groups. From the Table 11**,** it was clear that the C-N bond length was more or less same for all the groups. The expected C-N bond length was seen in all the cases. In the CdCl$_3$ tetrahedra group, a bond length of 2.429A° to 2.847A° was observed for all the Cd-Cl bonds in Table 12. Usually, the metal-halogen bonds are weaker and hence the bond length is higher. The Cd-Cl bond length was greater than C-H, C-N and C-C bond lengths. The hydrogen bonds present between the hydrogen of the methyl group and chlorine of the CdCl$_3$ group led to a stronger interaction between the Ar-N and CdCl$_3$.The structure of the title compound is [C$_6$H$_5$(CH$_3$)$_3$N]CdCl$_3$ as shown in Fig. 5. ORTEP plot structure was given in Fig. 6.
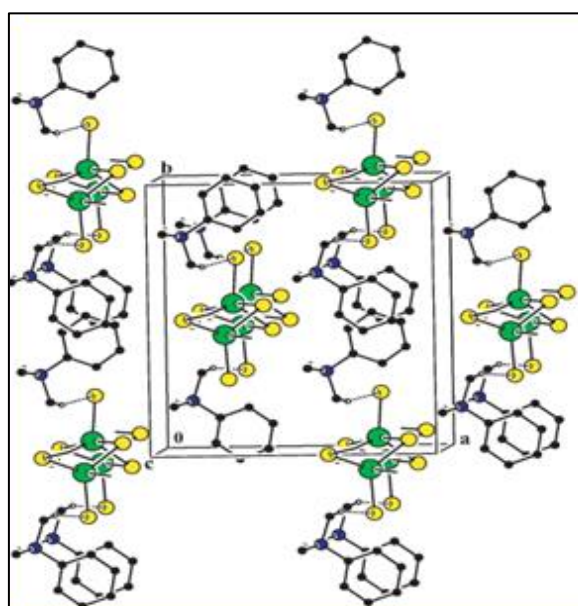

Fig. 6: ORTEP plot of PTMATCl – Cd (II) crystals

Table 6. Bond angles for N-C-H

Group	Bond angle (°)
N(1)-C(7)-H(7A)	109.5
N(1)-C(7)-H(7B)	109.5
N(1)-C(7)-H(7C)	109.5
N(1)-C(8)-H(8A)	109.5
N(1)-C(8)-H(8B)	109.5
N(1)-C(8)-H(8C)	109.5
N(1)-C(9)-H(9A)	109.5
N(1)-C(9)-H(9B)	109.5
N(1)-C(9)-H(9C)	109.5

Table 7. Bond angles for C-C-N

Group	Bond angle (°)
C(1)-C(6)-N(1)	118.4(12)
C(5)-C(6)-N(1)	120.9(12)

Table 8. Bond angles for C-C-C

Group	Bond angle (°)
C(6)-C(1)-C(2)	120.6(17)
C(3)-C(4)-C(5)	120.4(17)
C(4)-C(5)-C(6)	118.5(17)
C(1)-C(6)-C(5)	120.6(14)
C(4)-C(3)-C(2)	121.0(16)

Table 9. Bond angles for C-C-H

Group	Bond angle (°)
C(1)-C(2)-H(2)	120.6
C(2)-C(1)-H(1)	119.7
C(2)-C(3)-H(3)	119.5
C(3)-C(2)-H(2)	120.6
C(3)-C(4)-H(4)	119.8
C(4)-C(3)-H(3)	119.5
C(4)-C(5)-H(5)	120.7
C(5)-C(4)-H(4)	119.8
C(6)-C(5)-H(5)	120.7

Table 10. The Cl-Cd bond distance

Group	Bond angle (°)
C(6)-C(1)-C(2)	120.6(17)
C(3)-C(4)-C(5)	120.4(17)
C(4)-C(5)-C(6)	118.5(17)
C(1)-C(6)-C(5)	120.6(14)
C(4)-C(3)-C(2)	121.0(16)

Table 11. The C-C bond distance

Group	Bond angle (°)
C(6)-C(1)-C(2)	120.6(17)
C(3)-C(4)-C(5)	120.4(17)
C(4)-C(5)-C(6)	118.5(17)
C(1)-C(6)-C(5)	120.6(14)
C(4)-C(3)-C(2)	121.0(16)

Table 12. The C-H bond distance

Groups	Bond distance (A°)
C(1)-H(1)	0.93
C(2)-H(2)	0.93
C(3)-H(3)	0.93
C(4)-H(4)	0.93
C(5)-H(5)	0.93
C(7)-H(7A)	0.96
C(7)-H(7B)	0.96
C(7)-H(7C)	0.96
C(8)-H(8A)	0.96
C(8)-H(8B)	0.96
C(8)-H(8C)	0.96
C(9)-H(9A)	0.96
C(9)-H(9B)	0.96
C(9)-H(9C)	0.96

Table 13. The C-N and Cd-Cl bond distance

Group	Bond distance (o)
C(6)-C(1)-C(2)	120.6(17)
C(3)-C(4)-C(5)	120.4(17)
C(4)-C(5)-C(6)	118.5(17)
C(1)-C(6)-C(5)	120.6(14)
C(4)-C(3)-C(2)	121.0(16)
Group	Bond distance (o)
Cd(1)-Cl(2)#2	2.429(3)
Cd(1)-Cl(3)#1	2.657(3)
Cd(1)-Cl(1)#3	2.847(3)

4. CONCLUSION

Elemental analysis data obtained for the grown crystal have confirmed their molecular formula. The crystalline nature of the prepared compounds from aqueous solution has been confirmed by getting well-defined peaks at different 2θ values. The IR spectra were used to assign various vibrational frequencies due to different chemical bonds in these compounds. The IR spectra of all the compounds were similar and confirmed the presence of methyl and methylene groups in these compounds. The ^{1}H NMR spectra suggested the presence of aromatic and alkyl groups in these compounds. The TG-DTA thermogram indicated 100% decomposition of the compound. The observed emission peak with maximum intensity at 534 nm has shown that the crystal exhibited green colour fluorescence emission; also, the existence of only one sharp peak has indicated good crystalline perfection. The compound $[C_6H_5(CH_3)_3N]$ $CdCl_3$ crystallized with needle habits was transparent. The structure of the compound was determined as monoclinic with space group P2$_1$/n, the unit cell dimensions of a = 12.763 A^o, b =14.496 A^o and c = 7.136 A^o with Z=4. The co-ordination around Cd atom was tetrahedral. The structure of the compound has shown hydrogen bonds between chlorine and hydrogen of the phenyl groups. Further, it was concluded that the structure of phenyl trimethylammonium trichloro cadmiate (II) crystals were well- defined with the help of the mentioned spectral characterization and materials were having more thermal stability in nature. These compounds may be used for optical and industrial applications.

FUNDING

CONFLICTS OF INTEREST

The authors declare that there is no conflict of interest.

COPYRIGHT

REFERENCES

Asahi, T. and Hasebe, K., Measurement of monoclinic angle in the ferroelastic phase of [N(CH$_3$)$_4$]$_2$XBr$_4$(X=Zn, Co, Mn, Cd), *J. Phys. Soc. Jpn.*, 63(7), 2827-2828 (1994).
https://dx.doi.org/10.1143/JPSJ.63.2827

Dvorak, V. and Kind, R., On the low temperature phase in Rb$_2$Zncl$_4$, *Phys. Status Solidi B.*, 107, K109 (1981).
https://dx.doi.org/10.1002/pssb.2221070253

Fousek, J., Birefringence studies of A$_2$BX$_4$ compounds with incommensurate phases, *Phase Transit.*, 36(1-4), 165-190 (1991).
https://dx.doi.org/10.1080/01411599108203438

Gesi, K., Effect of hydrostatic pressure on te phase transitions in tetraethylammonium tetrahalogenometallic compounds, *Ferroelectrics,* 159(1), 49-54 (1986).
https://dx.doi.org/10.1080/00150199408007547

Hasebe, K., Mashiyama, H., Tanisaki, S. and Gesi, K., X – Ray study of the phase transitions in {N{CH$_3$}$_4$}$_2$ZnBr$_4$ and {N{CH$_3$}$_4$}$_2$CoBr$_4$, *J. Phys. Soc. Jpn.,* 53(5), 1866-1868 (1984).
https://dx.doi.org/10.1143/JPSJ.53.1866

Heine, V. and McConnel, J. D., The origin of incommensurate structures in insulators, *J. Physica C.,* 17(7), 1199-1205 (1984).
https://dx.doi.org/10.1088/0022-3719/17/7/014

Kahirizi, M. and Steinitz, M. O., Atructural phase transitions in ((C$_2$H$_5$)$_4$N)CdX$_4$ and ((CH$_3$)$_4$N)$_2$CdX$_4$ compounds with X = Cl, Br, *Solid State Commun.*, 70(6), 599-603 (1989).
https://dx.doi.org/10.1016/0038-1098(89)90357-8

Kapustianik, V., Sveleba, S., Dacko, S., Vajdanych, V. and Mokryi, V., Dielectric properties of trimethylammonium tetrachlorcobaltate crystals, *Phase Transit.*, 54, 131-136 (1995).
https://dx.doi.org/10.1080/01411599508213224

Kasano, H., Takashige, M. and Mashiyama, H., J., Structure study of paraelectric-ferroelectric transition in Monoclinic K_2ZnBr_4, *Phys. Soc. Jpn.*, 61(5), 1580 – 1584 (1992).
https://dx.doi.org/10.1143/JPSJ.61.1580

Mashiyama, H., Hasebe, K. and Tanisaki, S., X – ray diffraction study on the incommensurate – commensurate phase transitions in $\{N(CH_3)_4\}_2CoCl_4$, *J. Phy. Soc. Jpn.,* 49(4), 1633-1634 (1980).
https://dx.doi.org/10.1143/JPSJ.49.1633

Mohanraj, V., Pavithra, R., Thenmozhi, M. and Umarani, R., Synthesis, spectral, structural and thermal characterization of inorganic crystal : Phenyl trimethulammonium tetrachlorocobaltate, *Asian J. Chem*., 31(8), 1779-1784 (2019).
https://dx.doi.org/10.14233/ajchem.2019.21929

Peer Mohamed, M., Sudha, C., Jayaprakash, P., Vinitha, G., Nageswari, M., Sangeetha, P., Rathika ThayaKumari, C. and Lydia Caroline, M., Growth and characterization of L-histidinium fumarate fumaric acid monohydrate single crystal: A promising second and third order non linear optical material, *Chinese J Phys.*, 60, 581-597 (2019).
https://dx.doi.org/10.1016/j.cjph.2019.05.032

Sato, S., Ikeda, R. and Nakamura, D., Motions of tetramethylammonium cations and phase transitions in solid $[(CH_3)_4N]_2CdX_4$ (X = Cl, Br, I) as studied by ^1H NMR, powder X-ray diffraction and differential thermal analysis measurements, *Bull. Chem. Soc. Jpn.*, 59(6), 1981 (1986).
https://dx.doi.org/10.1246/bcsj.59.1981

Sawada, S., Shiroshi, Y., Yamamoto, A., Takashige, M. and Mantuso, M., Ferroelectricity in $\{N(CH_3)_4\}_2$ $CoCl_4$, *Phys. Lett.* A., 67(1), 56-58 (1978).
https://dx.doi.org/10.1016/0375-9601(78)90566-2

Shimomura, S., Fujii, Y. and Hamaya, N., Hydrostatic pressure effect on the ferroelastic monoclinic phase of $[N(CH_3)_4]_2MCl_4$ (M = Fe, Zn), *J. Phys. Soc. Jpn.,* 64(12), 4759-4765 (1995).
https://dx.doi.org/10.1143/JPSJ.64.4759

Strukov, B. A., Global hysteresis in ferroelectrics with incommensurate phases, *Phase Transit*., 15(2-3), 143-179 (1989).
https://dx.doi.org/10.1080/01411598908206844

Subashini, R. and Arjun, S., Synthesis and physicochemical properties of bis(L-asparaginato) zinc (II): A promising new semiorganic crystal with high laser damage threshold for shorter wavelength generation, *Opt. Laser Technol.,* 101, 248-256(2018).
https://dx.doi.org/10.1016/j.optlastec.2017.11.009